Taylor & Francis
Taylor & Francis Group

REPORT

🔓 OPEN ACCESS ✅ Check for updates

TNB-486 induces potent tumor cell cytotoxicity coupled with low cytokine release in preclinical models of B-NHL

Harbani K. Malik-Chaudhry [ID][a], Kirthana Prabhakar[a], Harshad S. Ugamraj[a], Andrew A. Boudreau [ID][a], Benjamin Buelow[a], Kevin Dang[a], Laura M. Davison[a], Katherine E. Harris[a], Brett Jorgensen[a], Heather Ogana[b], Duy Pham[a], Ute Schellenberger [ID][a], Wim Van Schooten[a], Roland Buelow[a], Suhasini Iyer[a], Nathan D. Trinklein[a], and Udaya S. Rangaswamy [ID][a]

[a]Teneobio, Inc., Newark, CA, United States; [b]Graduate Program in Cancer Biology and Genomics, Keck School of Medicine, University of Southern California, Los Angeles, CA, United States

ABSTRACT
The therapeutic potential of targeting CD19 in B cell malignancies has garnered attention in the past decade, resulting in the introduction of novel immunotherapy agents. Encouraging clinical data have been reported for T cell-based targeting agents, such as anti-CD19/CD3 bispecific T-cell engager blinatumomab and chimeric antigen receptor (CAR)-T therapies, for acute lymphoblastic leukemia and B cell non-Hodgkin lymphoma (B-NHL). However, clinical use of both blinatumomab and CAR-T therapies has been limited due to unfavorable pharmacokinetics (PK), significant toxicity associated with cytokine release syndrome and neurotoxicity, and manufacturing challenges. We present here a fully human CD19xCD3 bispecific antibody (TNB-486) for the treatment of B-NHL that could address the limitations of the current approved treatments. In the presence of CD19+ target cells and T cells, TNB-486 induces tumor cell lysis with minimal cytokine release, when compared to a positive control. *In vivo*, TNB-486 clears CD19+ tumor cells in immunocompromised mice in the presence of human peripheral blood mononuclear cells in multiple models. Additionally, the PK of TNB-486 in mice or cynomolgus monkeys is similar to conventional antibodies. This new T cell engaging bispecific antibody targeting CD19 represents a novel therapeutic that induces potent T cell-mediated tumor-cell cytotoxicity uncoupled from high levels of cytokine release, making it an attractive candidate for B-NHL therapy.

Introduction

B cell non-Hodgkin lymphoma (B-NHL) affects approximately 1.5 million patients worldwide and presents with diverse clinical manifestations dependent on the subtype. Among the major subtypes of B-NHL, diffuse large B cell lymphoma (DLBCL) and follicular lymphoma represent the most common aggressive and indolent subtypes of B-NHL, respectively, and together account for over 50% of all cases.[1] Chemotherapy coupled with Rituxan®, a monoclonal antibody (mAb) targeting CD20, has remained the first-line treatment for the majority of the subtypes. Despite a high overall response rate (>90%), most patients relapse and treatment of relapsed/refractory B-NHL remains a challenge owing to the complexity of the disease subtypes, patient characteristics and variable responses between subtypes to initial therapy.[2,3]

Based on the success of Rituxan®, lineage markers gained popularity as targets for the treatment of hematologic malignancies. CD19 is a B cell restricted surface receptor present on all B cells, including neoplastic B cells. The expression of CD19 is broader than CD20, from the pro-B cell to plasmablast stage, and is lost upon differentiation into plasma cells, making it a popular target for B cell malignancies.[4,5] Efforts to target CD19 have included multiple immunotherapy modalities such as mAbs and their derivatives, e.g., antibody-drug

conjugates (ADCs), T cell engaging bispecific antibodies (T-BsAbs), and chimeric antigen receptor (CAR)-T cells.[5–7] Of these, mAbs have shown limited success, likely owing to lower antigen density of CD19 on malignant B cells compared to CD20,[8] the inherently limited antibody-dependent cell-mediated cytotoxicity or complement-dependent cytotoxicity activities of mAbs, or rapid internalization of CD19 upon antibody crosslinking.[5] CD19-targeted ADCs have also faced hurdles due to toxicity associated with the cytotoxic payload or inhibition of internalization due to high CD21 expression.[9,10]

Immunotherapy modalities that harness the cytolytic potential of T cells to target and kill tumor cells, such as T-BsAbs or CAR-T cells have shown promise in the treatment of chemotherapy-resistant or relapsed hematologic malignancies. Blinatumomab (Blincyto®), an antibody-based Bispecific T cell Engager (BiTE) that targets CD3 and CD19, is approved by the U.S. Food and Drug Administration (FDA) for B cell acute lymphoblastic leukemia (B-ALL) and shows durable responses in relapsed/refractory DLBCL.[11,12] Axicabtagene ciloleucel (Yescarta®) and tisagenlecleucel (Kymriah®) are CD19 targeted CAR-T cell products that are FDA-approved as third-line therapies for B-NHL. However, both T-BsAbs and CAR-T cells have significant toxicity hurdles due to cytokine

---

release syndrome (CRS) and neurotoxicity,[13] which result in limited or modified dose regimens combined with clinical management of the toxicities.[14,15]

T-BsAbs that demonstrate efficient tumor cell cytotoxicity coupled with reduced cytokine release *in vitro* have been described and could prove beneficial in the clinic by reducing CRS-related toxicity.[16–18] Previous work from our group has highlighted a novel CD3-engaging arm which, when paired with a tumor-targeting arm, shows reduced cytokine secretion with comparable tumor cell lysis relative to a T-BsAb that contains a higher affinity anti-CD3 arm.[16]

This study describes TNB-486, a novel fully human CD19xCD3 bispecific antibody designed for the treatment of B-NHL. TNB-486 engages CD19 and CD3, leading to activation of resting polyclonal CD4+ and CD8+ T cells that result in efficient lysis of CD19+ tumor cells, but with markedly lower cytokine release. The preclinical characterization of TNB-486 presented here outlines the anti-tumor efficacy of TNB-486 in *in vitro, in vivo* and *ex vivo* models of B cell malignancies.

Results

CD19 expression on normal and malignant B cells

Cell surface expression of CD19 on tumor cell lines derived from various B cell malignancies was confirmed by flow cytometry. The number of CD19 molecules on the cell surface (antigen density) of multiple CD19-positive cell lines representing Burkitt's lymphoma (BL), DLBCL or ALL were quantified by flow cytometry analysis using a commercially available monoclonal CD19 antibody (Figure 1a). Similarly, CD19 expression was also determined on B cells in peripheral blood mononuclear cells (PBMCs) from healthy individuals, and PBMCs or dissociated tumor cells (DTCs) from chronic lymphocytic leukemia (CLL) or DLBCL patients (Figure 1b). The CD19 antigen density on tumor cell lines and patient-derived samples ranged from 6×10^3 to 161×10^3 and 8×10^3 to 98×10^3, respectively. In contrast, normal PBMCs had

a more uniform expression ranging between $21–32 \times 10^3$ CD19 molecules per cell (Figure 1b).

Generation and characterization of a CD19xCD3 bispecific antibody

Due to the complex extracellular structure of CD19,[19,20] protein-based immunization strategies have shown limited success, leading to low numbers of unique antibody clones against CD19. The handful of available clones are primarily derived from mouse hybridomas and require humanization.[21–23] Some humanized murine antibodies have a higher risk of immunogenicity in the clinic, and thus fully human antibodies are a preferred alternative. Fully human heavy-chain only antibodies targeting CD19 were generated by immunization of UniRats® followed by next-generation sequencing (NGS)-based antibody repertoire discovery approach.[24] A lead anti-CD19 UniAb® was identified by screening multiple candidates for cell surface binding to CD19+ tumor cells, as well as high-affinity binding to CD19 protein by Octet. Antibodies against CD3 were generated in OmniFlic® animals and have been previously described.[16,25]

T-BsAbs were generated by pairing the lead anti-CD19 V_H (variable heavy region of the antibody) with a high-affinity CD3-binding arm (as a Positive Control, PC) or a low-affinity CD3-binding arm (Lead antibody, TNB-486) using knobs-in-holes technology as previously described.[16] TNB-486 is a fully human asymmetric bispecific monoclonal IgG4 antibody. The structure is presented in Figure 2a. The PC T-BsAb that contains a high-affinity CD3-binding arm was used in all relevant experiments. A negative control antibody (NC) that contains the same anti-CD3 V_H as TNB-486 but an irrelevant tumor binding arm was used where applicable. TNB-486 shows robust expression, desirable biophysical properties, and low aggregation propensity after thermal stress (Table 1, Figure S1).

Cell binding dose curves of TNB-486 across a panel of CD19-positive and -negative cell lines are shown in Figure 2b. The EC_{50} of cell binding on the Daudi, Raji and Nalm-6
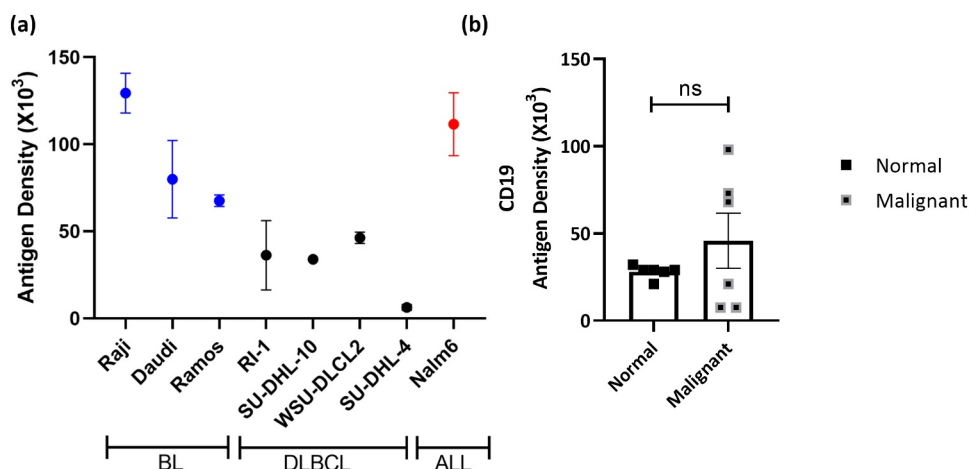
Figure 1. **CD19 Expression on normal and malignant B cells** (a) Antigen density of CD19 was measured on the indicated human B cell lines by quantitative flow cytometry. Error bars indicate standard error mean (SEM) of 2–4 independent experiments. (b) Antigen density of CD19 was enumerated on normal human PBMCs and malignant B cells from 4 CLL and 2 DLBCL DTCs or PBMCs. Error bars represent SEM of independent samples. Unpaired Student's t-test was used to determine significance.
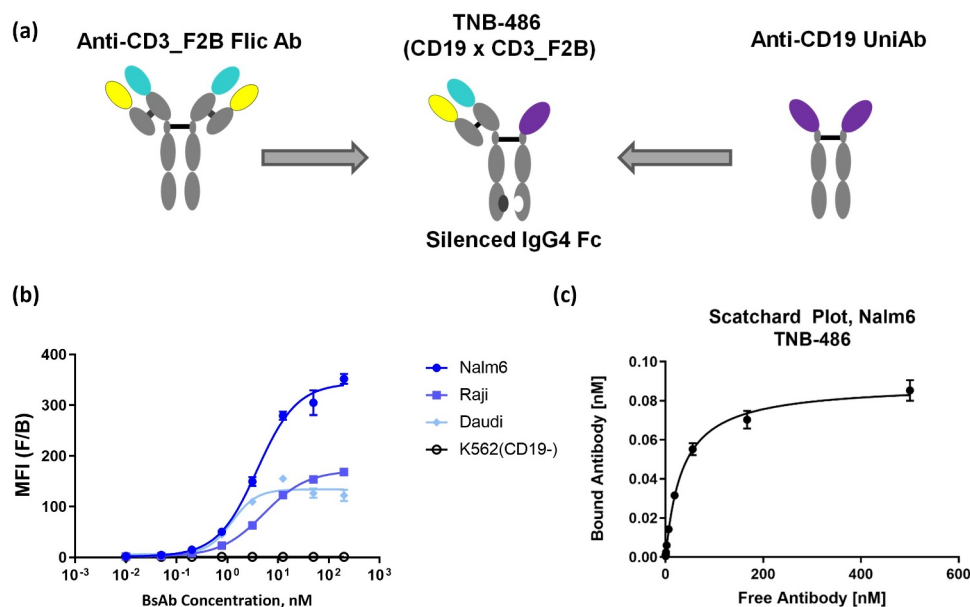
Figure 2. TNB-486 is a fully human bispecific antibody engaging CD19 and CD3 (a) TNB-486 was constructed using knobs-into-holes technology. The format of the antibody is depicted. (b) Cell binding dose curves of TNB-486 on three CD19+ B cell lines Daudi, Raji and Nalm-6, and one CD19- cell line, K562 is shown. (c) Cell surface affinity of TNB-486 to CD19 expressed on Nalm-6 cells was determined by Scatchard analysis.

Table 1. TNB-486 has favorable protein biophysical characteristics. Thermal stability of TNB-486 was assessed by determining the melting temperatures (T_{onset}, T_{m1} and T_{m2}). Further, aggregation propensity was assessed by SEC-UPLC before and after exposure to heat stress. Percent High Molecular Weight (%HMW) species are shown at T = 0 and after 30 days.

| Yield (g/L)	Thermal Stability (%HMW): 5°C		Thermal Stability (%HMW): 25°C		T_{onset} (°C)	T_{m1} (°C)	T_{m2} (°C)
	T_{d0}	T_{d30}	T_{d0}	T_{d30}			
3.3	0.5	0.5	0.5	0.5	57.4	67.7	76.9

cell lines ranged from 1.2 to 5.2 nM. The cell surface affinity of TNB-486 on target expressing cells was determined by Scatchard analysis. Consistent with EC_{50} values obtained in Figure 2b, the K_D of the anti-CD19 arm to Nalm-6 cells was 1.8 nM (± 0.54 nM). The binding of the anti-CD3 arm to human T cells has been previously published.[16]

In vitro functional assessment of TNB-486

The ability of TNB-486 to activate CD4+ and CD8+ T cells in the presence of CD19+ tumor cells was assessed by CD69 expression. Consistent with the mode of action of T-BsAbs, in the presence of CD19+ RI-1 tumor cells, TNB-486 activated both CD4+ and CD8+ T cells to a similar extent as the PC (Figure 3a). Approximately 95% of total CD8+ T cells and 55% of total CD4+ T cells were CD69+ following incubation of pan T cells with CD19+ RI-1 tumor cells at saturating concentrations of TNB-486. The EC_{50} of TNB-486-induced activation was 103.6 pM and 121.8 pM, for CD4+ and CD8+ T cells, respectively, compared to $EC_{50} \sim$ 1–2 pM for the PC in both T cell subtypes. In a similar assay setup that included an incubation time of 5 days, TNB-486 induced proliferation of CD4+ and CD8+ T cells to the same extent as the PC, but with a higher EC_{50} value (Figure 3b). The EC_{50}s for TNB-486-mediated proliferation was 62.9 pM among

CD4+ carboxyfluorescein succinimidyl ester (CFSE)+ T cell subset and 46.9 pM for CD8+ CFSE+ T cell subset, compared to EC_{50}s ≤ 1 pM for the PC. The NC did not mediate activation or proliferation of T cells, demonstrating target-dependent activation of T cells by TNB-486. In addition, TNB-486-mediated T cell activation was accompanied by the release of cytotoxic granules, perforin and granzyme B, in the supernatant of co-cultures of T cells and RI-1 tumor cells (Figure 3c). The maximum concentration of the cytotoxic granules release was similar to that of the PC. As expected, cytotoxic granule release coincided with flow-cytometry based measurements of tumor cell lysis in the co-culture assay (data not shown).

Since CD19 is expressed on both normal and neoplastic B cells, TNB-486 is expected to mediate lysis of normal B cells in peripheral blood. To test this, T cells and B cells sorted from PBMCs of healthy human donors were incubated with TNB-486 at a ratio of 10:1 and the depletion of B cells was evaluated over 4 days. By 24 hours of incubation, TNB-486 induced ~40% T cell-dependent cellular cytotoxicity (TDCC) of B cells in the culture. Percent lysis increased to 65% by 48 hours and reached over 90% by 96 hours. Of note, the EC_{50} of lysis did not vary substantially between 48 hours and 96 hours (EC_{50}s ranging from 0.93 to 1.35 nM) and therefore, all cytotoxicity experiments henceforth were performed at 48 hours (Figure 4a). Next, the TDCC of PBMCs from three independent donors was evaluated. Figure 4b shows that in the presence of TNB-486, autologous T cells can mediate lysis of B cells in the culture by 48 hours. In addition, compared to the PC, TNB-486 induced lower levels of interleukin (IL)-2, interferon (IFN)γ, IL-6, IL-10 and tumor necrosis factor (TNF) in the culture supernatant (Figure S2). To confirm that this time point was the most relevant for evaluating TDCC with CD19+ tumor cells as well, TDCC experiments were conducted by incubating TNB-486 with Nalm-6 CD19+ tumor cell line
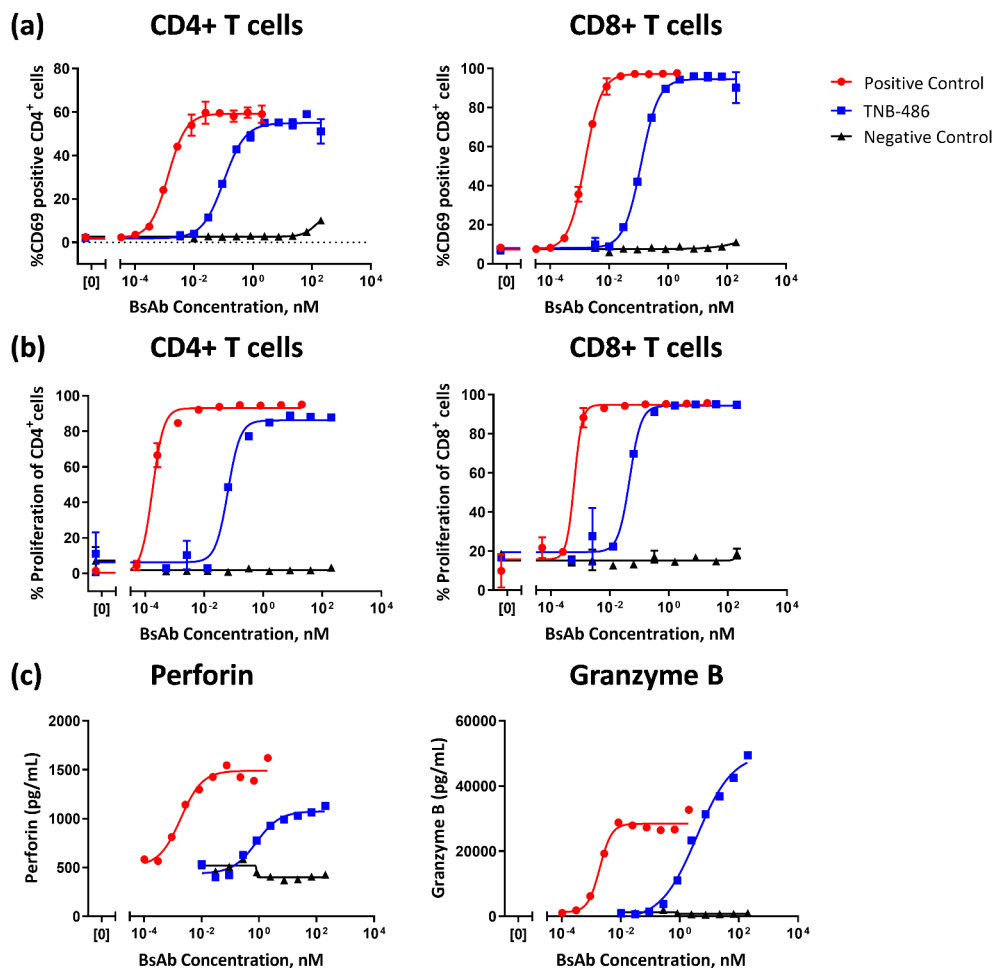
Figure 3. TNB-486 mediates T cell activation, proliferation, and cytotoxic granule release. CD19+ RI-1 tumor cells were incubated with T cells from a single healthy donor at an E:T ratio of 10:1 and serially diluted indicated test antibody (a) Activation of CD4+ or CD8+ T cells were determined by flow cytometric measurement of the activation marker CD69 after 24 hours of co-culture (b) T cell proliferation was measured by labeling T cells with CFSE and monitoring CD4 or CD8 proliferation after 5 days of co-culture (c) Perforin and granzyme B levels were measured in the cell culture supernatants of co-culture after 48 hours by ELISA.

with pan T cells from PBMCs. After 48 and 72 hours of co-culture, cytotoxicity and cytokine release were evaluated. While the maximum %cytotoxicity increases over time, the EC_{50} does not change between 48 and 72 hours (0.11 nM vs 0.18 nM for TNB-486 at 48 vs 72 hours, respectively) (Figure S3). TNB-486-mediated induction of IL-2 and IFNγ levels remained low at both timepoints (~100 pg/mL and 60 pg/mL of IL-2 at 48 and 72 hours, respectively; and ~600 pg/mL of IFNγ at both 48 and 72 hours). Based on this data, the 48-hour timepoint gives a conservative measure of cytokine release as well as cytotoxicity in this *in vitro* system and was used for further TDCC experiments.

To evaluate the T cell redirecting properties of TNB-486, TDCC experiments were performed by incubating TNB-486 in the presence of resting CD3+ human T cells and a variety of CD19+ tumor cells for 48 hours. At an effector to target ratio (E:T) of 5:1, TNB-486 induced concentration-dependent TDCC of multiple CD19+ tumor cell lines derived from leukemia or lymphoma origin, namely, Ramos, Daudi, Raji, Nalm-6, WSU-DLCL2, SU-DHL-4, or RI-1 (or RIVA). Among these, RI-1 is a DLBCL cell line known to be resistant to

rituximab,[26] and WSU-DLCL2 is derived from a patient with aggressive lymphoma and is resistant and refractory to chemotherapy agents.[27] The maximum average percent lysis induced by TNB-486 ranged from 35% to 82% between the different tumor cell lines (Figure 4c). In contrast, a concentration-dependent TDCC was not observed in the CD19- K562 tumor cell line, illustrating the specificity of TNB-486 to CD19 expressing tumor cells.

Upon treatment with T-BsAbs, both CD4+ and CD8+ T cells are known to contribute to cytotoxicity of tumor cells.[28] To assess this, TNB-486 was incubated with either CD4+ or CD8+ T cells in the presence of RI-1 tumor cells and cytotoxicity was measured at 48 hours. As shown in Figure 4d, cytotoxicity was observed when either CD4+ or CD8+ T cells were used as the source of effector cells. The maximal percent cytotoxicity induced by TNB-486 was similar when CD4+ or CD8+ cells were used as effectors (39.2% and 48.4% lysis, respectively) but lower than that of the PC (75.6% and 98.6%, respectively).

TNB-486 consistently mediated TDCC in PBMCs derived from several donors. In TDCC experiments with two different CD19+ tumor cells (RI-1 or Raji) and T cells from three independent donors, TNB-486 resulted in T-cell-mediated
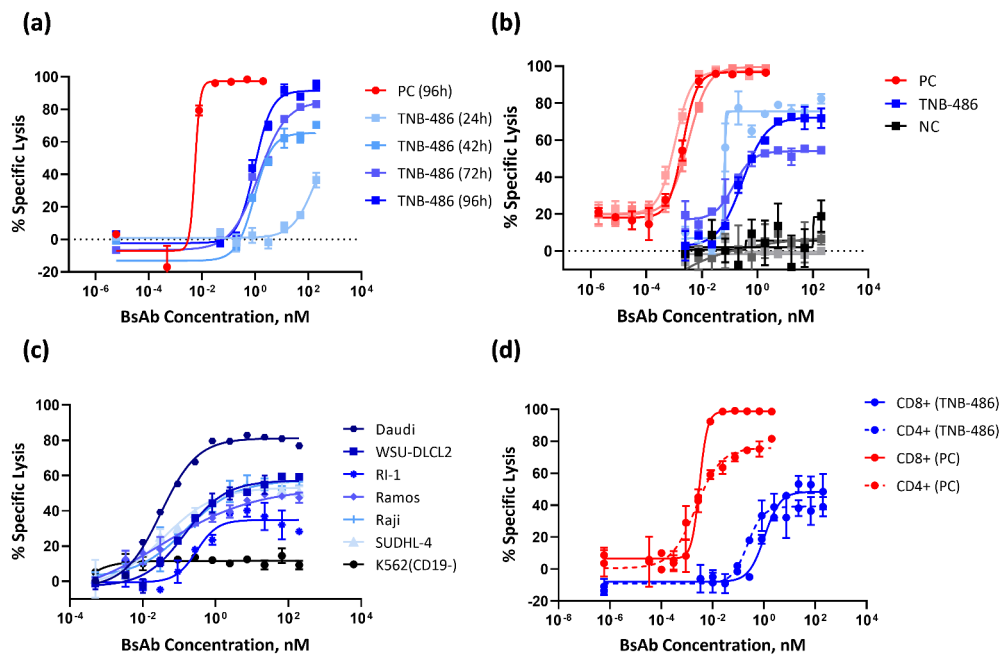
Figure 4. TNB-486 induces lysis of CD19+ B cells (a) T cells and B cells sorted from normal PBMCs were co-cultured at an E:T ratio of 10:1 and incubated with varying doses of TNB-486. Cytotoxicity of B cells was evaluated by flow cytometry at 24 h, 42 h, 72 h and 96 h. (b) PBMCs from three independent donors (the shades of blue represent three independent donors for TNB-486, shades of red and gray/black represent the three donors for PC and NC, respectively) were incubated with increasing doses of TNB-486 without adjusting the E:T ratio. Cytotoxicity of B cells was measured by flow cytometry at 48 h. (c) CD19+ tumor cells Daudi, Raji, Ramos, SU-DHL-4, WSU-DLCL2 and RI-1 or a CD19- K562 cell line were co-cultured with T cells from a healthy donor (at an E:T ratio of 5:1) and increasing doses of TNB-486. TDCC was measured at 48 hours by enumerating the live CD20+ B cells by flow cytometry (d) TNB-486 mediated cytotoxicity of CD19+ RI-1 tumor cells and CD4+ or CD8+ T cells as effectors was determined as in (C).

tumor cell lysis irrespective of the donor. The EC_{50}s of TNB-486 mediated cell lysis were 23.5 ± 11.5 pM or 0.9 ± 0.2 nM for Raji cells or RI-1, respectively, compared to that of the PC with an EC_{50} of 2.2 ± 2.5 pM in both cell lines. Importantly, at concentrations sufficient to achieve maximum tumor lysis, the levels of IL-2 induced by TNB-486 was markedly lower than that induced by the PC (Figure 5). IFNγ and TNF also displayed a similar trend where TNB-486 induced lower cytokine levels compared to the PC. IL-6 and IL-10 levels were similar between TNB-486 and PC, but with a markedly higher EC_{50} for TNB-486 (Table 2). In similar TDCC experiments with Raji tumor cells and T cells, TNB-486 was compared with blinatumomab and the PC. TNB-486 induced similar maximum percentage of lysis as that of blinatumomab, which was
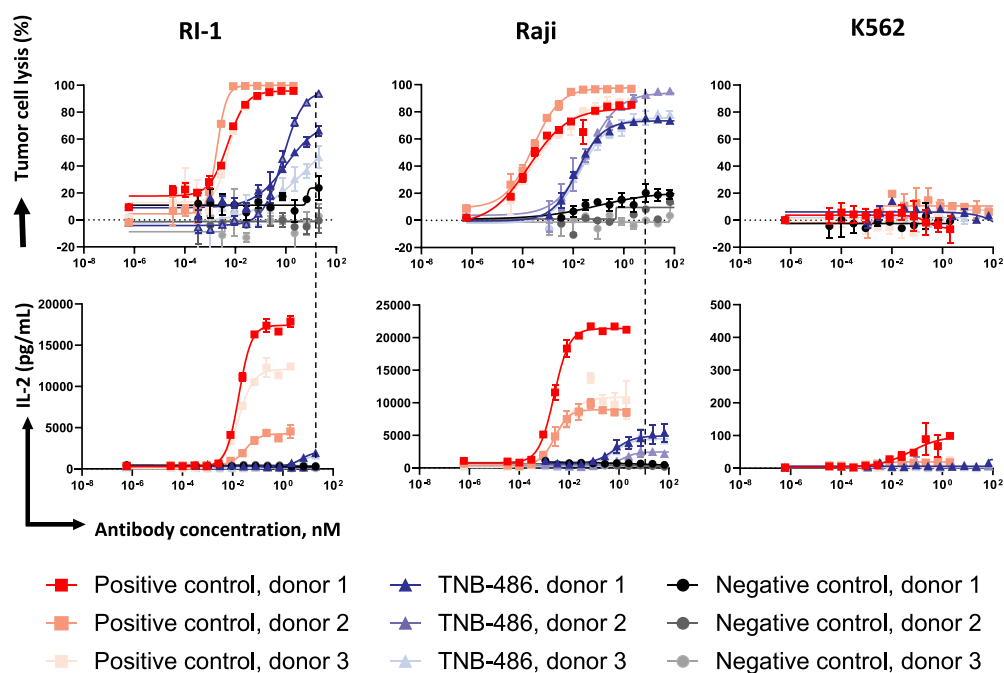

Figure 5. TNB-486 induced lysis is accompanied by low cytokine release. TDCC of TNB-486 was evaluated as in (Figure 4) but using T cells from three independent donors. Raji or RI-1 tumor cells were used as target cells. IL-2 levels were measured from culture supernatants of the co-culture assay by MSD.

Table 2. TNB-486 induces lower cytokine release compared to the PC. The TDCC of TNB-486 was assessed as described in Figure 5. Supernatants from the co-culture were used to measure cytokine release. The EC_{50}s of cytokine release are shown in Table 2(A) and the maximum cytokine released is shown in Table 2(B).

(A) EC_{50} values of dose curves for TNB-486 or PC mediated cytokines

	EC_{50} (pM), TNB-486						EC_{50} (pM), PC					
	RI-1			Raji			RI-1			Raji		
Target Cell												
Donor ID	D2546	D2921	D0628	D2546	D2921	D0628	D2546	D2921	D0628	D2546	D2921	D0628
IFNγ	1534	N/A	1411	N/A	2164	358	7	N/A	5	8	3	5
IL-2	5364	N/A	6192	N/A	1410	570	18	31	17	3	3	4
IL-6	3487	N/A	2961	N/A	N/A	N/A	15	N/A	10	N/A	N/A	N/A
IL-10	1423	735	1369	N/A	N/A	322	3	N/A	N/A	16	N/A	N/A
TNF	2620	708	3051	N/A	1225	490	18	14	13	1	2	N/A

(B) Maximum cytokine levels induced by TNB-486 or PC (related to Figure 5)

	Maximum Induction (pg/mL), TNB-486						Maximum Induction (pg/mL), PC					
	RI-1			Raji			RI-1			Raji		
Target Cell												
Donor ID	D2546	D2921	D0628	D2546	D2921	D0628	D2546	D2921	D0628	D2546	D2921	D0628
IFNγ	42492	13647	24080	18188	18373	6416	65646	22860	28701	80441	43053	17758
IL-2	2061	443	2094	4929	2456	4494	17874	4537	12430	21217	8567	10378
IL-6	246	3	193	39	47	19	1124	131	554	189	79	27
IL-10	1294	74	1804	326	56	213	1448	101	1795	910	99	360
TNF	1473	632	1372	742	500	500	8174	2533	4367	5747	1828	1159

similar to the PC used in this study, but with a higher EC_{50}. The equivalent cytotoxicity was accompanied by reduced cytokine secretion in TNB-486-treated samples compared to blinatumomab (Figure S4).

Evaluation of cytotoxicity in patient-derived samples was performed by obtaining either PBMCs or DTCs from B-CLL or DLBCL patients. Depletion of CD20 positive B cells was used as a readout for lysis. Depending on the number of viable cell numbers recovered from each of the frozen samples, the experiment was conducted with an adjusted E:T ratio of 10:1 or unadjusted E:T ratio. Data in Table 3 shows that TNB-486 induced the autologous T cell killing of >10% B cells in 6 of 8 samples tested.

Table 3. TNB-486 mediates lysis of tumor cells derived from leukemia or lymphoma patients. Lysis of CD19+ cells from ex vivo patient derived PBMCs or dissociated tumor cells (DTCs) was evaluated by flow cytometry. Average % lysis of tumor cells is shown.

Ex Vivo Sample Type	Effector: Target Ratio	CD19 Antigen Density (x10³)[d]	Average % lysis of tumor cells[e]
Lymphoma, NOS	1.707[b]	7.6	2.3[a]
NHL, Extranodal Marginal Zone B cell (MALT: Mucosa-Associated Lymphoid Tissue)	0.01[b]	NT	-1.4
NHL, Extranodal Marginal Zone B cell (MALT: Mucosa-Associated Lymphoid Tissue) PBMC	12.54[b]	20.7	55.7
NHL, Diffuse Large B cell Lymphoma	25.95[b]	7.6	25.4[a]
CLL PBMC	10[c]	70.3	18.2
CLL PBMC	10[c]	20.4	14.9
NHL	2[b]	-	28.2
CLL PBMC[f]	10[c]	97.9	44.4
	0.064[b]		17.5

[a]Assay incubation time was 24 hours
[b]Effector to target cell ratio was left unaltered
[c]Effector to target cell ratio was adjusted to indicated value
[d]Antibody used for antigen density estimate; Biolegend Cat#302208 Clone#HIB19
[e]Normalized to control samples without antibody
[f]Same sample was tested with and without modifying E:T ratio as indicated in column 2.

In vivo anti-tumor efficacy of TNB-486 in murine xenograft models

The *in vivo* anti-tumor efficacy of TNB-486 was assessed against human tumor cell lines xenografted into immunocompromised NOG (NOD.Cg-Prkdcscid IL2rgtm1Sug/JicTac) mice in three different models. In the first study using a disseminated model of Burkitt lymphoma, NOG mice were engrafted with luciferase-expressing Raji tumor cells and human PBMCs, followed by treatment with TNB-486. The doses of TNB-486 were 10 ng, 100 ng, 1 μg, or 10 μg per mouse (or 10 ng PC or 10 μg NC, respectively) administered intravenously (IV) every 5 days. Bioluminescent imaging was used to monitor tumor burden. After two treatments at the respective dose levels, TNB-486-treated animals showed a dose-dependent tumor reduction compared to the NC, which did not show any reduction in tumor growth (Figure 6a). At doses 100 ng, 1 μg, or 100 μg/mouse, TNB-486 cleared tumors similar to the PC at 10 ng/mouse. The 10 ng/mouse dose of TNB-486 showed tumor growth inhibition (TGI) at 8 days post-implantation (dpi), but the TGI was not sustained as seen at 14 dpi, indicating that higher doses of TNB-486 compared to the PC are required to achieve a similar efficacy, which is consistent with the *in vitro* TDCC experiments.

Efficacy was also measured in a xenograft model using the SU-DHL-10 (DLBCL) tumor cell line, where immunocompromised NOG mice received tumor cells subcutaneously, followed by PBMC engraftment and treatment with TNB-486. By day 40 post-implantation (pi), TNB-486 displayed a dose-dependent TGI (10.89%, 35.68% and 88.52%) with doses 1, 10, or 100 μg/animal, respectively, compared to the 100 μg/animal dose of PC, which resulted in a TGI of 90.74% (Figure 6b). In a similar subcutaneously injected tumor model using the Nalm-6 (ALL) cell line and resting PBMCs as the source of effector cells, TNB-486 treatment resulted in significant TGI at all doses by 35 dpi (79.36%, 94.99%, and 94.86% TGI, at doses 1, 10, or 100 μg/animal, respectively, compared to 55.86% TGI in the 100 μg/animal dose of PC) (Figure 6c). Interestingly, the
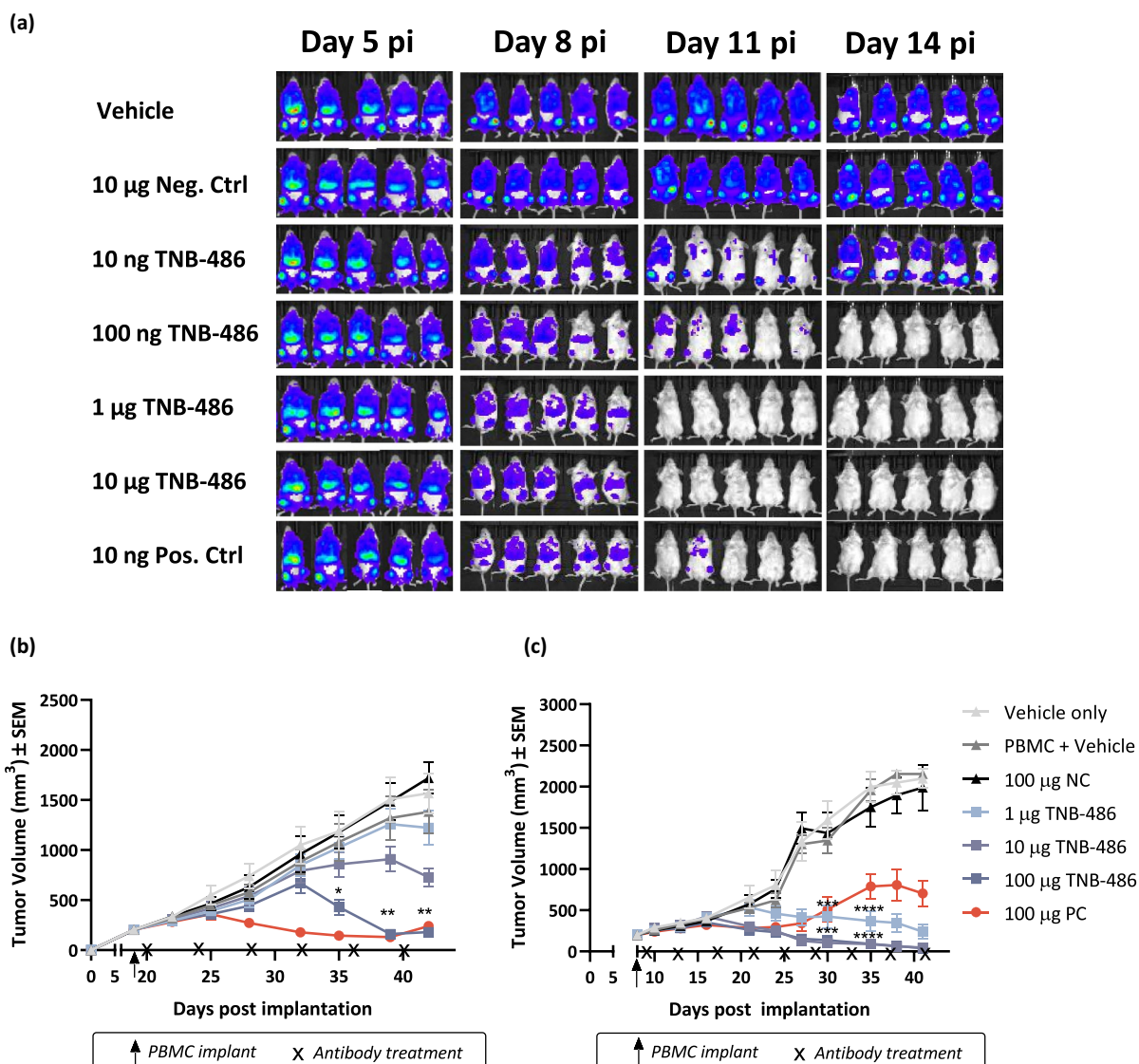
(a)

(b) **(c)**

Figure 6. **TNB-486 induces tumor regression in multiple xenograft models of established** *tumors.* (a) 1 × 10⁶ Raji-luc cells were injected *i.v* via tail vein into CIEA-NOG mice (N = 5/group). On *day 6 post-implantation (pi)*, 10 × 10⁶ human PBMCs were injected *i.v.* TNB-486, NC or PC, at the respective doses shown, was injected on days 7, 14 and 21. GvHD/GvT onset was observed by day 15 pi and hence data points after day 14 are not shown. (b and c) CIEA-NOG mice (N = 10/group) received 10 × 10⁶ SUDHL-10 cells (b) or Nalm-6 cells (c) with 50% Matrigel subcutaneously in the lower right flank. When tumor volume reached 200 mm3, mice received 10 × 10⁶ human PBMCs i. v followed by antibody treatment Q4D as shown in the figure. Statistical analyses were performed by Two-way ANOVA on GraphPad Prism. TNB-486 treated animals were compared with PBMC + vehicle treated animals. A value of p < .05 was considered significant.

PC showed reduced efficacy compared to TNB-486, suggesting that strongly activating anti-CD3 containing antibodies could allow relapse of tumor over time.

Pharmacokinetics (PK) of TNB-486 in non-human species

The PK of TNB-486 was evaluated in BALB/c mice following a single tail vein injection at 1 or 10 mg/kg. Non-compartmental analysis and two compartmental analyses showed that TNB-486 PK was linear across the dose ranges tested. Group mean clearance (CL) ranged from 13.0 to 15.5 mL/day/kg and group mean half-life ($t_{1/2}$) ranged from 2.6 to 4.1 days (Table 4). Since TNB-486 does not cross-react with CD19 or CD3 in rodent species, the observed linear PK was expected.

PK parameters in cynomolgus monkeys were similarly measured after a single IV bolus dose of 0.1, 1 or 10 mg/kg. CL ranged from 5.99 to 7.41 mL/day/kg and group mean terminal half-life ($t_{1/2}$) ranged from 11.4 to 12.9 days (Table 4). Although the anti-CD19 arm binds to cynomolgus monkey CD19, it did not affect TNB-486 PK in monkeys at the tested dose levels. Taken together, the observed linear PK in mice or monkeys is consistent with nonspecific clearance mechanisms dominating PK. Figures 7a and 7b show the serum concentrations of TNB-486 in mice and cynomolgus monkeys, respectively, at the specified doses. Cross-reactivity of the CD19 V_H to cynomolgus monkey B cells did not affect serum chemistry, PK or immune cell subset frequencies in the blood of cynomolgus monkeys (data not shown).

Table 4. The PK parameters of TNB-486 is similar to conventional antibodies. The PK parameters of TNB-486 were evaluated in mice or monkeys and the values are shown below.

Parameter	Units	Balb/c mice		Cynomolgus monkey		
		1 mg/kg	10 mg/kg	0.1 mg/kg	1 mg/kg	10 mg/kg
C_{max}	μg/mL	16.1	183	1.8	16.1	183
C_{max}/D	(μg/mL)/(μg/kg)	0.0161	0.018	0.018	0.0161	0.018
$t_{1/2}$	days	11.4	12.9	12	11.4	12.9
AUC_{inf}	μg/mL*days	168	1599	13.8	168	1599
AUC_{inf}/D	(μg/mL*days)/ (μg/kg)	0.17	0.16	0.14	0.17	0.16
% Extrap	%	41.9	41.4	32.6	41.9	41.4
CL	mL/day/kg	5.99	6.43	7.41	5.99	6.43
V_{ss}	mL/kg	95.6	121	116	95.6	121
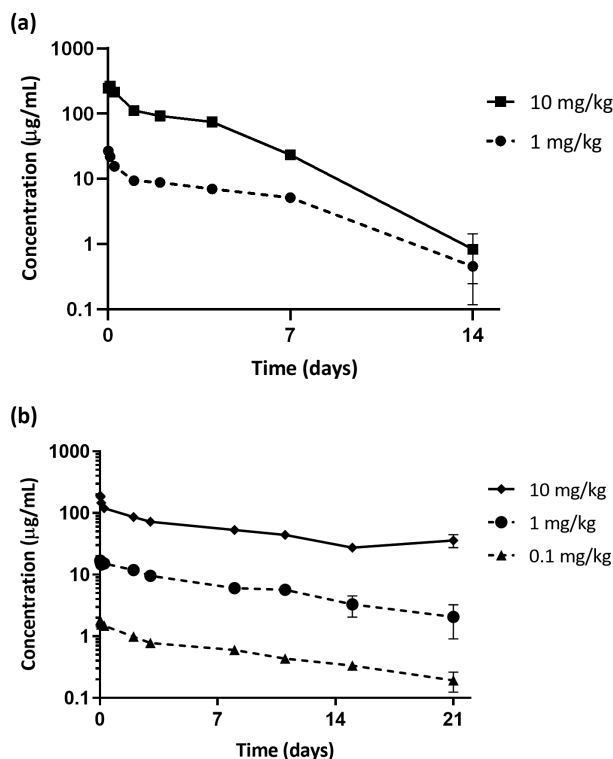
Figure 7. TNB-486 pharmacokinetics in mice and cynomolgus monkeys (a) PK parameters of TNB-486 was evaluated in normal Balb/c mice at 1 or 10 mg/kg (b) PK parameters of TNB-486 was evaluated in cynomolgus monkeys at 0.1, 1 or 10 mg/kg. Serum concentration of TNB-486 in mice were determined by an IgG4 specific AlphaLISA kit (mice) or antigen specific ELISA (cynomolgus monkeys).

Discussion

MAbs and derivatives such as ADCs targeting CD19 have been explored with limited clinical success. Rapid internalization of CD19 upon antibody binding limits the success of mAbs, and, in particular, ADCs have encountered challenges due to compensatory tumor evasion mechanisms.[6,9] T cell redirecting bispecific antibodies such as TNB-486 rely on cross-linking of T cells and target-expressing cells, thereby clustering T cell receptors (TCRs) to initiate a signaling cascade that results in activation, proliferation and cytokine/cytotoxic granule release by the T cells to lyse target cells.[29] This polyclonal and Major Histocompatibility Complex (MHC)-independent activation of T cells overcomes common evasion mechanisms used by cancer cells, such as down modulation of peptide-MHC antigen presentation or loss of antigenic epitopes.

Current CD19 targeting T cell therapies such as T-BsAbs/BiTEs and CAR-Ts are efficacious in the treatment of B cell malignancies, but have drawbacks such as CRS and neurotoxicity,[7,30,31] in addition to other challenges related to dosing of BiTEs or accessibility of CAR-Ts. Another tumor evasion mechanism with CD19-targeted CAR-Ts is antigen loss associated with exon skipping.[32,33] This appears to be likely due to immune pressure from long-term persistence of immunostimulatory domain-containing CAR-Ts compared to BiTEs.[34] In contrast, there was no CD19 loss observed in patients refractory to blinatumomab, a BiTE targeting CD19 and CD3.[35] The approval of blinatumomab has validated the T-BsAb approach for targeting CD19 in certain subsets of B cell lymphomas, but safety concerns have limited its use beyond ALL.[36] Of note, a CD19xCD3 T-BsAb was halted in development due to severe adverse events, including a Grade 5 adverse event related to neurotoxicity and/or CRS likely resulting from over-stimulation of T cells arising from the high-affinity engagement of CD3.[37,38] Therefore, safer off-the shelf T cell redirecting therapies targeting CD19 will change the course of therapies available for B-NHL.

Approaches to mitigate or manage CRS in current T-BsAb-based therapies generally belong to two categories: 1) Development of a newer-generation of T-BsAbs that intrinsically lower cytokine release compared to existing molecules; or 2) Mitigation of CRS in the clinic by step-dosing,[39] or management of CRS with anti-cytokine mAbs and, corticosteroids.[14,40] While the latter method is the most used currently, next-generation T-BsAbs using CD3 binding domains optimized for low cytokine release and reduced toxicity without compromising efficacy show substantial promise in the clinic.[41,42]

Novel anti-CD3 antibodies or affinity engineering of existing anti-CD3 antibodies have been generated by our group and others, respectively.[16,17,42] While affinity modification of the anti-CD3 arm can result in reduced cytokine release,[17] it is also possible that such engineering can result in unexpected immunogenicity or loss of binding specificity due to additional mutations introduced in the CDR.[43] TNB-486 is a fully human bispecific antibody derived from novel humanized rats without a need for humanization via CDR grafting. This could reduce the immunogenicity risk in humans compared to other rodent-derived antibodies that require humanization. The CD3 binding moiety in TNB-486 has shown similar activity when combined with a BCMA (B cell maturation antigen) binding arm where efficient tumor cell lysis is accompanied by minimal cytokine

release.[16] Similar to our BCMAxCD3 molecule, TNB-486 displayed efficient tumor cell lysis in multiple experimental formats, but did so while inducing lower levels of the cytokines IL-2, IFNγ, IL-6, IL-10 and TNF compared to a PC with a higher affinity anti-CD3 arm (Figure 4, 5 and Table 2 and Trinklein et al.).[16] The ability of TNB-486 to induce in vitro TDCC of multiple CD19+ cell lines derived from different subtypes of lymphoma cells, namely Burkitt's lymphoma, DLBCL, leukemia, including two cell lines that are refractory to chemotherapy (WSU-DLCL2) or rituximab (RI-1), suggests that TNB-486 has the potential to treat R/R B-NHL.[26,27]

Cytotoxicity induced via the perforin-granzyme pathway accounts for the majority of T cell-mediated target cell killing induced by T-BsAbs.[44] Consistent with this mechanism, TNB-486 induced the secretion of perforin and granzyme B in vitro, confirming the predominant mode of action of TNB-486-induced cytotoxicity. Interestingly, release of perforins and granzymes is similar between the PC and TNB-486, but cytokine production by TNB-486 is greatly reduced (Figure 5). The decoupling of cytokine release from cytotoxicity has been described in the context of pMHC-TCR complex formation at the T cell and target cell interface.[45] Cytotoxic T lymphocytes (CTLs) exposed to very low pMHC densities result in equivalent target cell cytotoxicity compared to those exposed to high pMHC densities, but are unable to induce cytokine secretion. This dual activation threshold determines the duration and the successful formation of a mature immunological synapse, which is critical for efficient T cell-mediated cytokine release, but not for T cell-mediated cytotoxicity.[46,47] Likewise, we believe that low-affinity engagement of CD3 by TNB-486 mirrors an immature immunological synapse with polarized lytic granule release and cytotoxicity, but is delayed in forming a complete synapse or unable to do so, thereby resulting in reduced cytokine release. In a previous study, the F2B anti-CD3 arm, the F1F anti-CD3 arm (used in PC) and clone OKT3, a widely used anti-CD3 antibody clone, were evaluated for their ability to bind to CD3ε, CD3δε or CD3γε heterodimers. It was shown that the F1F- and F2B-containing CD3 binding molecules bind to CD3δε but not CD3γε, whereas OKT3 binds to both CD3δε and CD3γε heterodimers. Additionally, F1F-containing antibodies can bind cynomolgus T cells, whereas F2B-containing antibodies cannot.[16] Therefore, the efficient cytotoxicity combined with low cytokine release appears to be a feature unique to the F2B-containing T-BsAbs and is likely due to a combination of the low affinity and a potential novel epitope. Studies to fully dissect the mechanism of decoupling cytokine release from cytotoxicity at a cellular level are underway.

Although CD8+ T cells are known to be the most effective at mediating T cell-dependent cytotoxicity owing to their ability to store preformed cytolytic granules such as perforin and/or granzyme, CD4+ T cells also induce cytotoxicity, albeit in a delayed manner.[26,36,37] Accordingly, TNB-486-mediated lysis occurred by recruitment of both CD4+ and CD8+ T cells to a similar extent (Figure 4c), whereas the positive control induced a higher percentage of lysis when CD8+ T cells were used. Along with the potent anti-tumor efficacy and low cytokine release, the linear PK and longer in vivo half-life of TNB-486 (Figure 7a, 7b and Table 1) could translate to a lower frequency and ease of dosing in the clinic compared to blinatumomab, which requires continuous IV infusion with a pump over multiple days depending on dosing regimen.[48]

The low magnitude of cytokine release observed in the TDCC experiments with TNB-486 differentiates it from other T-BsAbs and shows promise as a safer alternative to molecules co-targeting CD19 and CD3 that have high rates of CRS in the clinic. In addition to the safety issues arising from CRS, there is also a higher incidence of neurotoxicity associated with T cell-based therapies that target CD19.[15,49] Currently, it is unclear whether neurotoxicity is attributed to on-target toxicity or to damage caused by excessive CRS. Since neurotoxicity is observed in patients treated with CAR-Ts and T-BsAbs specific for targets such as CD20, CD22, and BCMA,[50–53] it appears to be more likely that CRS plays a critical role in neurotoxicity. There is also considerable evidence that CD19-targeted neurotoxicity is driven by hyperinflammation arising from CRS and the resulting disruption of the blood-brain barrier.[54,55] Therefore, efforts to mitigate CRS would also indirectly reduce incidence of associated neurotoxicity, making TNB-486 an attractive candidate for treatment of B cell malignancies. Historically, combination therapies have been shown to be most effective in cancers. Therefore, safer, and efficacious T cell engagers will allow combinations with other existing treatments to further improve the B-NHL treatment landscape.

In conclusion, the results shown in this work demonstrate that TNB-486 binds CD19 and CD3, resulting in depletion of CD19-expressing cells in preclinical models with minimal cytokine release. The low cytokine release profile suggests that TNB-486 could have a wider therapeutic window compared to other CD19xCD3 T-BsAbs in the clinic or in development. In addition, TNB-486 may have a more favorable dosing schedule owing to the longer half-life compared to single-chain variable fragment-based T-BsAbs. The anti-tumor efficacy in multiple models, low cytokine release, and favorable pharmacokinetics together strongly support the testing of TNB-486 in clinical trials for the treatment of B cell malignancies.

Materials and methods

Immunizations, next-generation sequencing, clonotype analysis and cloning

Methods used for immunization, NGS analysis and cloning were previously described in Harris et al.[25] Briefly, UniRat™ animals were immunized using Titermax/Ribi or Complete Freund's Adjuvant in combination with recombinant protein antigens (Antibody Solutions, CA, USA) in a 48-day protocol or genetic immunizations (Aldevron and MfD Diagnostics GmbH, Freiburg, Germany). For protein immunizations, animals received boosts of 10 μg of recombinant protein injected into each leg with the appropriate adjuvant. In the case of genetic immunizations, gold particles were coated with vectors containing cDNA of the target antigen, which were subsequently administered with a gene gun subcutaneously every 7 days. Plasma samples were collected to assess serum titers against the antigen by Enzyme-Linked Immunosorbent Assay (ELISA).

After approximately 7 weeks (protein antigen) or 10 weeks (DNA antigen) of immunization, total RNA was isolated from the

draining lymph nodes of each animal. Ig heavy chain sequences were amplified using first-strand cDNA synthesis and 5′ RACE by Polymerase Chain Reaction, following methods previously described in Harris et al.,[25] and then purified by gel extraction.

Next-generation sequencing was completed using the MiSeq platform (Illumina) with 2×300 paired-end reads. Indexing labels were added by primer extension to enable multiplexing of samples. Approximately 100,000 paired reads covered each sample, and those that showed alignment of less than 20 nucleotides to a human Ig locus were discarded. The merged forward and reverse reads of V_H regions were translated into open-reading frames. Subsequently, the framework and CDR regions were identified using IGBLAST (https://www.ncbi.nlm.nih.gov/igblast/). Agglomerative clustering was used to define clonotypes (defined by CDR3 protein sequences with at least 80% sequence similarity) within the samples. CDR3 clonotypes were ranked by the percent of total reads in a sample defined by that clonotype. The clonotypes with the greatest abundance were prioritized for high-throughput cloning into an expression vector containing a CH1-deleted human IgG1 Fc region. The resulting plasmids were validated by Sanger sequencing. Plasmids were transformed into *E. coli* grown in Luria-Bertani (LB) culture media and then purified to enable transient transfection of HEK 293 cells in 96-well format. After of expression, supernatants containing antibody were harvested and clarified by centrifugation.

Tumor cell lines

Nalm6 (catalog# CRL-3273), Raji (catalog# CCL-86), Daudi (catalog# CCL-213), Ramos (catalog# CRL-1596), K562 (catalog# CCL-243), SU-DHL-4 (catalog# CRL-2957) and SU-DHL-10 (catalog# CRL-2963) were purchased from American Type Culture Collection (ATCC) and maintained as per vendor's instructions. RI-1 (catalog # ACC 585) and WSU-DLCL2 (catalog# ACC 575) were purchased from DSMZ (German Collection of Microorganisms and Cell Cultures GmbH) and maintained as per vendor's instructions. All cell lines except K562 were grown in complete media containing Roswell Park Memorial Institute (RPMI)-1640 + 10% fetal bovine serum (FBS) + 1% PenStrep. K562 cell line was grown in Iscove's Modified Dulbecco's Medium+ 10% FBS + 1% PenStrep. All cells were grown at 37°C and 8% CO_2.

Cell binding by flow cytometry

Clarified supernatants from 96-well transfections containing antibodies or purified antibodies were evaluated for cell binding by flow cytometry. All washes and dilutions of cells, antibodies, and reagents were performed using flow buffer (1X phosphate-buffered saline (PBS), 1% bovine serum albumin (BSA), 0.1% NaN3, pH 7.4). Staining was performed in a round-bottom 96-well plate (Corning) seeded at 100,000 cells/well and all incubations were performed at 4°C or on ice. CD19+ tumor cells were incubated for 30 minutes with pre-diluted test antibodies (-curves) or 1:5 diluted HEK 293 supernatants containing antibodies (for primary screens) in a total volume of 50 μL. The cells were washed twice with 200 μL flow buffer. The cells were then

incubated for 30 minutes with detection antibody (Goat F(ab')2 Anti-Human IgG-PE, Southern Biotech catalog # 2042–09) at a final concentration of 0.625 μg/mL in flow buffer. Following two washes, the cells were resuspended in a final volume of 150 μL of flow buffer. The cells were analyzed on a BD FACSCelesta or a Guava easyCyte 8-HT flow cytometer. At least 3000 events were collected, and phycoerythrin (PE) geometric mean fluorescence intensity was plotted as a fold over background represented by cells incubated with secondary detection antibody only.

Expression and purification of CD19xCD3 bispecific antibody

TNB-486, PC and NC were expressed in ExpiCHO cells, according to manufacturer's instructions (Thermo Fisher Scientific, high titer protocol). Clarified supernatants were harvested and affinity purified using CaptureSelect™ CH1-XL resin (Thermo Fisher Scientific). Antibodies were further purified by anion exchange (Q Sepharose Fast Flow, Cytiva ID) to remove any product-related impurities. All proteins were analyzed by size exclusion chromatography-ultra-high performance liquid chromatography (SEC-UPLC) and sodium dodecyl sulfate Polyacrylamide Gel Electrophoresis to confirm their size and purity.

Biophysical characterization (T_m, T_{onset})

The thermal denaturation experiment was performed using Capillary- Differential scanning calorimetry (DSC). Briefly, a temperature ramp of 1°C was performed from 20°C to 120°C and a 16 sec filtering period. DSC scans were analyzed using MicroCal Origin® software. After subtraction of the respective buffer scan, protein scans were normalized against the protein concentration. The T_{onset} (the temperature that immediately precedes the protein unfolding event), was manually determined. Non two-state peak fitting was used to determine the T_m values and to calculate the enthalpies for each peak present in the normalized scans.

Thermal stress and stability characterization

TNB-486 was concentrated to 10 mg/mL in 20 mM citrate and 0.1 M NaCl pH 6.2. Presence of high molecular weight species (%HMW) was determined by SEC-UPLC before and after temperature stress (1 month at 37°C).

Quantification of CD19 expression

To estimate antibodies bound per cell (ABC), cell lines were stained at a saturating concentration of commercially available PE-labeled anti-CD19 antibody and tested via flow cytometry using BD Quantibrite beads as per manufacturer's instructions (BD catalog # 340495). Briefly, a PE-labeled CD19 antibody (BioLegend, clone HIB19) was used to establish saturating dose curves on the indicated cells. To generate the calibration curve, the BD Quantibrite calibration beads were also run on the flow cytometer, using the same settings used to acquire the cells. A standard curve was obtained by

plotting log (Molecules of Equivalent Soluble Fluorochrome) vs log (Mean Fluorescent Intensity) of the beads. Using the dose-dependent mean fluorescent intensity values for the antibody and the linear regression equation obtained from the Quantibrite PE beads, the number of PE-conjugated antibodies bound to each cell, ABC was determined by extrapolation of the standard curve. Estimated antigen density (or CD19 molecules per cell) was obtained by multiplying ABC values by 2.[56]

Calculation of cell surface affinity by Scatchard plot

Cell surface affinity of TNB-486 to human CD19 was assessed using an ALL cell line expressing human CD19 (Nalm6). Antibodies bound per cell was determined as described earlier using Alexa Fluor 488-labeled TNB-486 (Alexa Fluor labeling kit by Thermo Fisher Scientific), and Bangs Lab Quantum™ Alexa Fluor® 488 was used for generating the standard curve. To calculate affinity of the molecule (K_D), antibodies bound per cell was determined and used to further calculate free TNB-486 concentration using the formula:
$$[Starting TNB - 486] - [Bound TNB - 486] = [Free TNB - 486].$$

Isolation of PBMCs

PBMCs were isolated from peripheral blood leukapheresis pack (StemCell Technologies) using standard Ficoll-Paque PLUS reagent (GE healthcare) as per manufacturer's instructions. PBMCs were cryopreserved in CryoStor® freezing media (StemCell Technologies) in liquid nitrogen tanks until required for further analysis.

For isolation of T cell subsets of B cells, PBMCs isolated by the Ficoll-Paque method described earlier were removed from liquid nitrogen storage and thawed in a bead bath set at 37°C. The cells were transferred dropwise into a 50 mL conical centrifuge tube containing culture media (RPMI-1640 + 10% FBS+ 1% PenStrep) and recovered by centrifugation at 500 x g for 10 minutes at room temperature. The PBMCs were then resuspended in culture medium (RPMI-1640 + 10% FBS + 1% PenStrep) and proceeded for T cell isolation either immediately or after resting overnight at 37°C in a CO_2 buffered incubator. CD3+ T cells were isolated by negative selection using the Pan T cell isolation kit (Miltenyi) as per manufacturer's protocol. CD4+ or CD8+ subsets were isolated from pan T cells by negative selection microbeads for CD8+ or CD4+, respectively. B cells were isolated form thawed and/or rested PBMCs using the Pan B cell isolation kit (Miltenyi). For some *ex vivo* sample cytotoxicity assays, the B-CLL cell isolation kit was used (Miltenyi) as per manufacturer's protocol.

In vitro cytotoxicity assays

TDCC was determined by flow cytometric analysis of live CD20-positive tumor cells after 48 hours of co-culture with Pan T cells (Effector:Target is 5:1). After incubation, the supernatant was aliquoted into 96-well plates and stored at −80°C until needed for cytokine analysis by MesoScale Discovery (MSD). The cells were stained with Near Infrared(IR) Live/Dead marker (Thermo Fisher Scientific, 1:1000) and/or with human TrueStain Fc block (BioLegend, 1:20) followed by staining for different lineage markers with fluorescently labeled antibodies (BioLegend, anti-CD20 (clone 2H7), anti-CD8a (clone RPA-T8) and anti-CD4 (clone OKT4), 5 ul/test). After incubation, cells were washed with flow buffer (1X PBS + 1% BSA + 0.1% NaN$_3$) and resuspended at 1.00E+06 cells/mL in flow buffer. Equal volume of CountBright absolute counting beads (Invitrogen) was added to each well for uniform sample acquisition on a BD FACSCelesta flow cytometer. FlowJo™ version 10.6 was used for data analysis. To determine the percent of specific lysis of CD19+ B cells in normal cells, previously frozen PBMCs were thawed and incubated with serially diluted test antibodies without adjusting the E:T ratio. The averaged count of live CD20-positive tumor cells from the wells without antibody was used to set the background value. The percent of specific lysis was calculated as follows: percent specific lysis = (live target cell number without BsAb − live target cell number with BsAb)/(live target cell number without BsAb) × 100. To measure CD19+ B cell lysis over a time course of 24, 48, 72 and 96 hours, isolated pan T cells were used as effector cells and isolated B cells from the same donor were used as target cells at a E: T ratio of 10:1 and incubated with serially diluted test antibodies. The averaged count of live CD20-positive tumor cells from the wells without antibody was used to set the background value. The percent of specific lysis was calculated as described above.

Ex vivo cytotoxicity assay

The ability of TNB-486 to kill CD19+ tumor cells from CLL or DLBCL patient-derived samples (Discovery Life Sciences and IQ Biosciences) was determined by flow cytometric analysis of live CD20-positive cells after incubation for 24 or 48 hours in culture media. Cytotoxicity of TNB-486 is measured at 200 nM and the effector:target cell ratio was either set to 10:1 or left unchanged. The cells were stained with Near IR Live/Dead marker (Thermo Fisher Scientific, 1:1000) and with human TruStain Fc block (BioLegend, 1:20) followed by staining for different lineage markers with fluorescently labeled antibodies (BioLegend, anti-CD20 (clone 2H7), anti-CD8a (clone RPA-T8) and anti-CD4 (clone OKT4)). After incubation, cells were washed with flow buffer (1X PBS + 1% BSA + 0.1% NaN$_3$) and resuspended in 100 μL flow buffer. Samples were acquired on BD FACSCelesta flow cytometer and analyzed using FlowJo™ version 10.6.

Measurement of cytokines

Measurement of cytokines from the supernatant of *in vitro* TDCC assays or from serum of cynomolgus monkeys in the PK study was performed with the MSD U-plex platform. The preparation of standards and samples were performed as per manufacturer's instructions (MSD U-plex platform, cat# K15067L-4 and K15068L-2) and analyzed on a Meso Quickplex SQ 120 instrument.

Measurement of cytotoxic granules

Measurement of granzyme B and perforin from the supernatant of samples and preparation of standards were performed as per manufacturers' instructions (Invitrogen, Cat#BMS2027 and Cell Sciences Cat# CDK102A, respectively). The day prior to measuring perforin, the capture antibody was prepared in 1X PBS and

100 μL was seeded into each well of a Nunc flat-bottom 96-well plate (Invitrogen), covered with adhesive and stored at 4°C. All other reagents are provided in the kits inclusive of substrate solution and stop solution. The absorbance was read at 450 nm as the primary wavelength and 620 nm as the reference wavelength on a SpectraMax i3X plate reader (Molecular Devices).

Activation and proliferation of T cells

To measure activation of CD4+ and CD8+ T cells, isolated Pan T cells were incubated with diffuse large B cell lymphoma cells, RI-1 (E:T is 10:1), in the presence of TNB-486, positive control or negative control antibodies for 20 hours at 37°C and 8% CO_2. After incubation, cells were stained with fluorescently labeled antibodies for CD8 (clone RPA-T8), CD4 (clone OKT4) and CD69 (clone FN50). To determine activation of T cells, the percent increase in CD69-positive population was measured by flow cytometry. Proliferation assay setup is similar except the isolated T cells were first labeled with 2 μM CFSE dye (Invitrogen) before co-culturing with RI-1 cells and test articles for 5 days. Proliferation was determined by calculating the %CFSE positive proliferating CD8+ and CD4+ T cells by BD FACSCelesta flow cytometer.

In vivo efficacy studies

Disseminated mouse xenograft efficacy study

Each immune-compromised female Central Institute for Experimental Animals- NOG (NOD.Cg-Prkdcscid IL2rgtm1Sug/JicTac) (CIEA-NOG) mouse (4–5 weeks, Taconic Biosciences) was injected IV via tail vein with 1×10^6 Raji-luc cells (Aragen Biosciences Inc). On day six post-implantation (pi), each mouse was adoptively transferred IV with 1×10^7 PBMCs from a single donor (StemCell Technologies). On day seven, the mice were randomized into six treatment groups or one control group that received equivalent volume of the vehicle. All six treatment groups contained 5 animals each and each animal received the following dose per injection: 1) 10 μg NC, 2) 10 ng PC, 3) 10 ng TNB-486. 4) 100 ng TNB-486, 5) 1 μg TNB-486, or 6) 10 μg TNB-486.Test article (TNB-486, PC or NC) was injected every 5 days (Q5D) on days 6, 11 and 16 in the respective groups and at respective doses. Bioluminescent imaging and body weight measurements were determined every 3 days for 3 weeks.

Subcutaneous mouse xenograft efficacy studies

CIEA-NOG mice (5–7 weeks, Taconic Biosciences) were subcutaneously injected with 10×10^6 SU-DHL-10 or Nalm-6 with 50% Matrigel in lower right flank. When tumor volume reached 200 mm³, the mice were randomized into seven groups. Group one did not receive any PBMCs or drug treatment (group 1 – vehicle only). Groups 2–7 were adoptively transferred IV with 1×10^7 PBMCs (StemCell Technologies) from a single donor. One day after PBMC injection, test article or vehicle was injected into each animal in groups 2–7 as follows: 2) vehicle, 3) 100 μg NC, 4) 1 μg TNB-486, 5) 10 μg TNB-486, 6) 100 μg TNB-486, or 7) 100 μg PC. Test article or vehicle was injected every 4 days in the respective groups and at respective doses for a total of 6 treatments. Twice per week, the length and width of each tumor were measured with digital calipers in two perpendicular dimensions, and the tumor volume was calculated using this formula: $(width^2 \times length)/2$. Clinical signs and body weight were also assessed twice per week. The murine studies were performed in accordance with protocols approved by the Aragen Bioscience's Institutional Animal Care and Use Committee (IACUC).

Mouse PK evaluation

The PK of TNB-486 was evaluated in BALB/c mice. 18 male BALB/c mice were administered a single tail vein injection of 1 or 10 mg/kg of TNB-486 (n = 3/group * 6 groups). Serum samples were collected for 14 days post-dose at set times ranging from 30 minutes to 14 days. Serum TNB-486 concentrations were measured by Perkin Elmer's Human Immunoglobulin G subclass 4 Pharmacokinetic Kit (Cat# AL304 C) as per manufacturer's instructions. PK parameters were estimated using Phoenix WinNonlin version 7.0 software (Pharsight Corp). 2-compartmental analysis was used to determine the PK of TNB-486 at each dose level.

Cynomolgus PK evaluation

The PK of TNB-486 was evaluated in nine female cynomolgus monkeys following a single IV bolus dose of 0.1, 1 or 10 mg/kg dose (Altasciences Preclinical Seattle LLC). Serum samples were collected for 21 days post-dose at set times ranging from 30 minutes to 21 days. Serum TNB-486 concentrations were measured by an antigen-based ELISA. 3 μg/mL of recombinant huCD19-His (Acro Biosystems Cat# CD9-H52H2) was coated onto a 96-well, Nunc MaxiSorp™ flat-bottom plate (Thermo Fisher Scientific, Cat# 44–2404-21). Plates were sealed and incubated overnight at 4°C, protected from light. After overnight incubation, plates were washed 3 times with 180 μL of wash buffer (Tris-Buffered Saline + 0.05% tween20). Wash supernatant was removed completely after the final wash step, and 200 μL of assay buffer (wash buffer + 1% milk w/v) was added as a blocking reagent. Plates were sealed and then incubated at room temperature for 1 hour and subsequently washed 6 times with 180 μL of wash buffer. After washing, 100 μL of reference standard or sample analytes diluted in assay buffer were added to each well and incubated at room temperature for 2 hours. After another wash cycle with 9 washes, 100 μL of 1 μg/mL of an anti-idiotypic antibody against anti-CD3 of TNB-486 (CD3_F2B_antiID, generated by Teneobio) was added and incubated for 30 minutes at room temperature. Following 9 washes, 100 μL of 1:5000 diluted mouse anti-Rat IgG2a-HRP was added as a detection reagent (Southern Biotech Cat# 3065–05) and was incubated for 15–20 minutes at room temperature. Following this incubation and a wash cycle with 9 washes, 100 μL of Ultra 3,3′,5,5′-Tetramethylbenzidine (TMB) ELISA Substrate (Thermo Fisher Scientific cat# 34028) was added until a blue color developed (1–2 minutes). 100 μL of 2 N sulfuric acid was added to stop the reaction prior to absorbance measurements on a plate reader (SpectraMax i3X, Molecular Devices). The concentration of TNB-486 in the samples are directly proportional to absorbance values at 450 nm and were interpolated from a four-parameter logistic curve fit of the standard curve. PK parameters were estimated using Phoenix WinNonlin version 7.0 software (Pharsight Corp).

2-compartmental analysis was used to determine the PK of TNB-486 at each dose level.

Disclosure statement

All authors are current or former employees of Teneobio, Inc. with equity interests.

ORCID

Harbani K. Malik-Chaudhry (iD) http://orcid.org/0000-0002-2804-2697
Andrew A. Boudreau (iD) http://orcid.org/0000-0002-0016-4561
Ute Schellenberger (iD) http://orcid.org/0000-0002-4809-9383
Udaya S. Rangaswamy (iD) http://orcid.org/0000-0002-3994-3861

Author contributions

U.S.R., H.K.M.C., N.D.T., K.P., and H.S.U. contributed to the study design, analysis of results and manuscript preparation; NGS-based repertoire analysis was completed by N.D.T., K.H., and A.A.B.; molecular biology was conducted by K.H., L.M.D., K.D., and H.O.; U.S., H.K.M.C., B.J., and H.S.U. contributed to expression, purification and biophysical characterization of antibodies; lead discovery experiments, namely ELISAs and cell binding flow cytometry assays were designed and run by K.H., H.O., K.D., D.P., and U.S.R; U.S.R., and K.P., designed and executed *in vitro* cell-based assays; H.K.M.C., N.D.T., S.I., B.B., and W.v.S. contributed to the design and analysis of *in vivo* experiments; B.B., D.P., H.K.M.C., U.S.R., and K.P. contributed to the planning and execution of *ex vivo* experiments; U.S.R., H.K.M.C., and K.P., prepared figures; B.B., U.S., S.I., W.v.S, and R.B. contributed to data analysis and critical review of the data; the manuscript was written by U.S.R., H.K.M.C., and K.P.; all authors read and approved the submitted version.

List of abbreviations.

µg	Microgram
µL	Microliter
µM	Micromolar
ABC	Antibody Bound per Cell
ADC	Antibody-Drug Conjugate
ALL	Acute Lymphoblastic Leukemia
AUC$_{inf}$	Area Under the Curve from Zero to Infinity
B-ALL	B cell Acute Lymphoblastic Leukemia
BCMA	B cell Maturation Antigen
BiTE	Bispecific T cell Engager
B-NHL	B cell Non-Hodgkin's Lymphoma
BSA	Bovine Serum Albumin
BsAb	Bispecific Antibody
CAR-T	Chimeric Antigen Receptor T cells
CD	Cluster of Differentiation
CDR	Complementarity-Determining Regions
CFSE	Carboxyfluorescein Succinimidyl Ester
CH1	Constant Heavy Chain 1

(Continued)

(Continued).

CIEA	Central Institute for Experimental Animals
CL	Clearance
CLL	Chronic Lymphoblastic Leukemia
C$_{max}$	Maximum Serum Concentration
CO$_2$	Carbon dioxide
CRS	Cytokine Release Syndrome
CTL	Cytotoxic T Lymphocyte
DLBCL	Diffuse Large B Cell Lymphoma
dpi	Days Post Implantation
DTC	Dissociated Tumor Cells
E:T	Effector:Target
EC$_{50}$	Half Maximal Effective Concentration
ELISA	Enzyme Linked Immunosorbent Assay
FBS	Fetal Bovine Serum
Fc	Fragment Crystallizable
FDA	Food and Drug Administration
g	Grams
IACUC	Institutional Animal Care and Use Committee
IFN	Interferon
IL	Interleukin
IR	Infrared
IV	Intravenous
K$_D$	Equilibrium Dissociation Constant
kg	Kilogram
L	Liter
M	Molarity
mAb	Monoclonal Antibody
mg	Milligram
MHC	Major Histocompatibility Complex
mL	Milliliter
mM	Millimolar
MSD	Meso Scale Discovery
N	Normality
NaCl	Sodium chloride
NaN$_3$	Sodium Azide
NC	Negative Control
ng	Nanogram
NGS	Next-Generation Sequencing
nM	Nanomolar
nm	Nanometer
NOD	Non-Obese Diabetic
NOG	NOD.Cg-Prkdcscid IL2rgtm1Sug/JicTac
ns	Not Significant
PBMC	Peripheral Blood Mononuclear Cell
PBS	Phosphate-Buffered Saline
PC	Positive Control
PE	Phycoerythrin
pg	Picogram
pi	Post Implantation
PK	Pharmacokinetics
pM	Picomolar
pMHC	peptide-Major Histocompatibility Complex
Q5D	Every 5 Days
RACE	Rapid Amplification of cDNA Ends
RPMI	Roswell Park Memorial Institute
SD	Standard Deviation
SEC	Size Exclusion Chromatography
SEM	Standard Error Mean
t$_{1/2}$	Half-Life
T-BsAb	T cell-engaging Bispecific Antibody

(Continued)

(Continued).

TCR	T cell Receptor
TDCC	T cell Dependent Cellular Cytotoxicity
TGI	Tumor Growth Inhibition
T_m	Melting Temperature
TNF	Tumor Necrosis Factor
T_{onset}	Onset Temperature
UPLC	Ultra Performance Liquid Chromatography
V_H	Variable Domain
V_{SS}	Volume of distribution at Steady State

Ethics statement

PBMCs from healthy, deidentified donors were isolated from leukapheresis pack (StemCell Technologies). Human PBMCs were collected in accordance with scientific, ethical, and regulatory guidelines. Animal studies were carried out in accordance with the recommendations in the Guide for the Care and Use of Laboratory Animals of the National Institutes of Health. Rat maintenance and immunizations were carried out by certified animal facilities in the U.S. (Antibody Solutions, Sunnyvale, CA) and Germany (Aldevron and MfD Diagnostics GmbH, Freiburg, Germany) in accordance with national and international guidelines, with protocols reviewed by IACUC boards in the U.S. and comparable government boards in Germany. Mouse and cynomolgus monkey PK studies as well as mouse xenograft studies were performed by AAALAC accredited facilities following internal approval by their IACUC boards (Aragen Biosciences; Altasciences Preclinical Seattle LLC).

References

1. Swerdlow SH, Campo E, Pileri SA, Harris NL, Stein H, Siebert R, Advani R, Ghielmini M, Salles GA, Zelenetz AD, et al. The 2016 revision of the World Health Organization classification of lymphoid neoplasms. Blood. 2016;127(20):2375–90. doi:10.1182/blood-2016-01-643569.
2. Chaudhari K, Rizvi S, Syed BA. Non-Hodgkin lymphoma therapy landscape. Nat Rev Drug Discov. 2019;18(9):663–64. doi:10.1038/d41573-019-00051-6.
3. Hagemeister F. Rituximab for the Treatment of Non-Hodgkin's Lymphoma and Chronic Lymphocytic Leukaemia. Drugs. 2010;70 (3):261–72. doi:10.2165/11532180-000000000-00000.
4. Blanc V, Bousseau A, Caron A, Carrez C, Lutz RJ, Lambert JM. SAR3419: an Anti-CD19-maytansinoid immunoconjugate for the treatment of B-cell malignancies. Clin Cancer Res. 2011;17 (20):6448–58. doi:10.1158/1078-0432.CCR-11-0485.
5. Naddafi F, Anti-CD DF. 19 monoclonal antibodies: a new approach to lymphoma therapy. Int J Mol Cell Med. 2015;4:143–51.
6. Hammer O. CD19 as an attractive target for antibody-based therapy. mAbs. 2012;4(5):571–77. doi:10.4161/mabs.21338.
7. Watkins MP, Bartlett NL. CD19-targeted immunotherapies for treatment of patients with non-Hodgkin B-cell lymphomas. Expert Opin Investig Drugs. 2018;27(7):601–11. doi:10.1080/13543784.2018.1492549.
8. Horna P, Nowakowski G, Endell J, Boxhammer R. Comparative assessment of surface CD19 and CD20 expression on B-cell lymphomas from clinical biopsies: implications for targeted therapies. Blood. 2019;134(Supplement_1):5345–5345. doi:10.1182/blood-2019-129600.
9. Ingle GS, Chan P, Elliott JM, Chang WS, Koeppen H, Stephan J-P, Scales SJ. High CD21 expression inhibits internalization of anti-CD19 antibodies and cytotoxicity of an anti-CD19-drug conjugate. Br J Haematol. 2008;140(1):46–58. doi:10.1111/j.1365-2141.2007.06883.x.
10. Wolska-Washer A, Robak T. Safety and tolerability of antibody-drug conjugates in cancer. Drug Saf. 2019;42 (2):295–314. doi:10.1007/s40264-018-0775-7.
11. Topp MS, Kufer P, Gökbuget N, Goebeler M, Klinger M, Neumann S, Horst H-A, Raff T, Viardot A, Schmid M, et al. Targeted therapy with the t-cell–engaging antibody blinatumomab of chemotherapy-refractory minimal residual disease in b-lineage acute lymphoblastic leukemia patients results in high response rate and prolonged leukemia-free survival. J Clin Oncol. 2011;29 (18):2493–98. doi:10.1200/JCO.2010.32.7270.
12. Goebeler M-E, Bargou R. Blinatumomab: a CD19/CD3 bispecific T cell engager (BiTE) with unique anti-tumor efficacy. Leuk Lymphoma. 2016;57(5):1021–32. doi:10.3109/10428194.2016.1161185.
13. Maude SL, Barrett D, Teachey DT, Grupp SA. Managing Cytokine Release Syndrome Associated With Novel T Cell-Engaging Therapies. Cancer J Sudbury Mass. 2014;20(2):119–22. doi:10.1097/PPO.0000000000000035.
14. Lee DW, Gardner R, Porter DL, Louis CU, Ahmed N, Jensen M, Grupp SA, Mackall CL. Current concepts in the diagnosis and management of cytokine release syndrome. Blood. 2014;124 (2):188–95. doi:10.1182/blood-2014-05-552729.
15. Dholaria BR, Bachmeier C, Locke F. Mechanisms and Management of Chimeric Antigen Receptor T-Cell Therapy Related Toxicities. BioDrugs Clin Immunother Biopharm Gene Ther. 2019;33:45–60.
16. Trinklein ND, Pham D, Schellenberger U, Buelow B, Boudreau A, Choudhry P, Clarke SC, Dang K, Harris KE, Iyer S, et al. Efficient tumor killing and minimal cytokine release with novel T-cell agonist bispecific antibodies. mAbs. 2019;11(4):639–52. doi:10.1080/19420862.2019.1574521.
17. Zafra CLZD, Fajardo F, Zhong W, Bernett MJ, Muchhal US, Moore GL, Stevens J, Case R, Pearson JT, Liu S, et al. Targeting Multiple Myeloma with AMG 424, a Novel Anti-CD38/CD3 Bispecific T-cell–recruiting Antibody Optimized for Cytotoxicity and Cytokine Release. Clin Cancer Res. 2019;25(13):3921–33. doi:10.1158/1078-0432.CCR-18-2752.
18. Baliga R, Li K, Manlusoc M, Hinton PR, Ng DC, Tran MH, Shan B, Lu H, Saini A, Rahman S, et al. Abstract 5664: a bispecific IgM antibody format for enhanced T cell dependent killing with minimal cytokine release. Cancer Res. 2020;80(16 Supplement):5664–5664.
19. Lobner E, Wachernig A, Gudipati V, Mayrhofer P, Salzer B, Lehner M, Huppa JB, Kunert R. Getting CD19 Into Shape: expression of Natively Folded "Difficult-to- Express" CD19 for Staining and Stimulation of CAR-T Cells. Front Bioeng Biotechnol. 2020;8:49. doi:10.3389/fbioe.2020.00049.
20. Teplyakov A, Obmolova G, Luo J, Gilliland GL. Crystal structure of B-cell co-receptor CD19 in complex with antibody B43 reveals an unexpected fold. Proteins. 2018;86(5):495–500. doi:10.1002/prot.25485.
21. Meeker TC, Miller RA, Link MP, Bindl J, Warnke R, Levy R. A unique human B lymphocyte antigen defined by a monoclonal antibody. Hybridoma. 1984;3(4):305–20. doi:10.1089/hyb.1984.3.305.
22. Ghetie MA, Picker LJ, Richardson JA, Tucker K, Uhr JW, Vitetta ES. Anti-CD19 inhibits the growth of human B-cell tumor lines in vitro and of Daudi cells in SCID mice by inducing cell cycle arrest. Blood. 1994;83(5):1329–36. doi:10.1182/blood. V83.5.1329.1329.
23. Zola H, MacArdle PJ, Bradford T, Weedon H, Yasui H, Kurosawa Y, et al. Preparation and characterization of a chimeric CD19 monoclonal antibody. Immunol Cell Biol. 1991;69(Pt 6):411–22.
24. Clarke SC, Ma B, Trinklein ND, Schellenberger U, Osborn MJ, Ouisse L-H, Boudreau A, Davison LM, Harris KE, Ugamraj HS, et al. Multispecific antibody development platform based on human heavy chain antibodies. Front Immunol. 2018;9:3037. doi:10.3389/fimmu.2018.03037.
25. Harris KE, Aldred SF, Davison LM, Ogana HAN, Boudreau A, Brüggemann M, Osborn M, Ma B, Buelow B, Clarke SC, et al. Sequence-based discovery demonstrates that fixed light chain human transgenic rats produce a diverse repertoire of

antigen-specific antibodies. Front Immunol. 2018;9:889. doi:10.3389/fimmu.2018.00889.

26. Due H, Brøndum RF, Young KH, Bøgsted M, Dybkær K. MicroRNAs associated to single drug components of R-CHOP identifies diffuse large B-cell lymphoma patients with poor outcome and adds prognostic value to the international prognostic index. BMC Cancer. 2020;20(1):237. doi:10.1186/s12885-020-6643-8.

27. Al-Katib AM, Smith MR, Kamanda WS, Pettit GR, Hamdan M, Mohamed AN, Chelladurai B, Mohammad RM, et al. Bryostatin 1 down-regulates mdr1 and potentiates vincristine cytotoxicity in diffuse large cell lymphoma xenografts. Clin Cancer Res Off J Am Assoc Cancer Res. 1998;4(5):1305–14.

28. Porakishvili N, Kardava L, Jewell AP, Yong K, Glennie MJ, Akbar A, Lydyard PM. Cytotoxic CD4+ T cells in patients with B cell chronic lymphocytic leukemia kill via a perforin-mediated pathway. Haematologica. 2004;89:435–43.

29. Wu Z, Cheung N-KV. T cell engaging bispecific antibody (T-BsAb): from technology to therapeutics. Pharmacol Ther. 2018;182:161–75. doi:10.1016/j.pharmthera.2017.08.005.

30. Teachey DT, Rheingold SR, Maude SL, Zugmaier G, Barrett DM, Seif AE, Nichols KE, Suppa EK, Kalos M, Berg RA, et al. Cytokine release syndrome after blinatumomab treatment related to abnormal macrophage activation and ameliorated with cytokine-directed therapy. Blood. 2013;121(26):5154–57. doi:10.1182/blood-2013-02-485623.

31. Maloney DG. Anti-CD19 CAR T cell therapy for lymphoma — off to the races! Nat Rev Clin Oncol. 2019;16(5):279–80. doi:10.1038/s41571-019-0183-7.

32. Asnani M, Hayer KE, Naqvi AS, Zheng S, Yang SY, Oldridge D, Ibrahim F, Maragkakis M, Gazzara MR, Black KL, et al. Retention of CD19 intron 2 contributes to CART-19 resistance in leukemias with subclonal frameshift mutations in CD19. Leukemia. 2020;34 (4):1202–07. doi:10.1038/s41375-019-0580-z.

33. Orlando EJ, Han X, Tribouley C, Wood PA, Leary RJ, Riester M, Levine JE, Qayed M, Grupp SA, Boyer M, et al. Genetic mechanisms of target antigen loss in CAR19 therapy of acute lymphoblastic leukemia. Nat Med. 2018;24(10):1504–06. doi:10.1038/s41591-018-0146-z.

34. Jacoby E. Relapse and Resistance to CAR-T Cells and Blinatumomab in Hematologic Malignancies. Clin Hematol Int. 2019;1(2):79–84. doi:10.2991/chi.d.190219.001.

35. Jabbour E, Düll J, Yilmaz M, Khoury JD, Ravandi F, Jain N, Einsele H, Garcia-Manero G, Konopleva M, Short NJ, et al. Outcome of patients with relapsed/refractory acute lymphoblastic leukemia after blinatumomab failure: no change in the level of CD19 expression. Am J Hematol. 2018;93(3):371–74. doi:10.1002/ajh.24987.

36. Bukhari A, Lee ST. Blinatumomab: a novel therapy for the treatment of non-Hodgkin's lymphoma. Expert Rev Hematol. 2019;12 (11):909–18. doi:10.1080/17474086.2019.1676717.

37. Affimed Places Cancer Immunotherapy Candidate AFM11 on Clinical Hold after Patient Death [Internet]. GEN - Genet. Eng. Biotechnol. News2018 [cited 2020 Dec 11]; Available from: https://www.genengnews.com/news/affimed-places-cancer-immunotherapy-candidate-afm11-on-clinical-hold-after-patient-death/

38. Reusch U, Duell J, Ellwanger K, Herbrecht C, Knackmuss SH, Fucek I, Eser M, McAleese F, Molkenthin V, Gall FL, et al. A tetravalent bispecific TandAb (CD19/CD3), AFM11, efficiently recruits T cells for the potent lysis of CD19(+) tumor cells. mAbs. 2015;7(3):584–604.

39. Bartlett NL, Sehn LH, Assouline SE, Bosch F, Magid Diefenbach CS, Flinn I, Hong J, Kim WS, Matasar MJ, Nastoupil LJ, et al. Managing cytokine release syndrome (CRS) and neurotoxicity with step-fractionated dosing of mosunetuzumab in relapsed/refractory (R/R) B-cell non-Hodgkin lymphoma (NHL). J Clin Oncol. 2019;37 (15_suppl):7518–7518. doi:10.1200/JCO.2019.37.15_suppl.7518.

40. Le RQ, Li L, Yuan W, Shord SS, Nie L, Habtemariam BA, Przepiorka D, Farrell AT, Pazdur R. FDA approval summary: tocilizumab for treatment of chimeric antigen receptor t cell-induced severe or life-threatening cytokine release syndrome. Oncologist. 2018;23(8):943–47. doi:10.1634/theoncologist.2018-0028.

41. Teneobio, Inc. A Multicenter, Phase 1, Open-label, Dose-escalation and Expansion Study of TNB-383b, a Bispecific Antibody Targeting BCMA in Subjects With Relapsed or Refractory Multiple Myeloma. clinicaltrials.gov. 2020. Available from: https://clinicaltrials.gov/ct2/show/NCT03933735.

42. TNB383B.0001: A Multicenter, Phase 1, Open-Label, Dose-Escalation And Expansion Study of TNB-383B, a Bispecific Antibody Targeting BCMA in Subjects with Relapsed or Refractory Multiple Myeloma. Blood American Society of Hematology.

43. Harding FA, Stickler MM, Razo J, DuBridge RB. The immunogenicity of humanized and fully human antibodies. mAbs. 2010;2 (3):256–65. doi:10.4161/mabs.2.3.11641.

44. Renner C, Held G, Ohnesorge S, Bauer S, Gerlach K, Pfitzenmeier J-P, Pfreundschuh M. Role of perforin, granzymes and the proliferative state of the target cells in apoptosis and necrosis mediated by bispecific-antibody-activated cytotoxic T cells. Cancer Immunol Immunother CII. 1997;44(2):70–76. doi:10.1007/s002620050357.

45. Irvine DJ. Function-specific variations in the immunological synapses formed by cytotoxic T cells. Proc Natl Acad Sci. 2003;100(24):13739–40. doi:10.1073/pnas.2536626100.

46. Purbhoo MA, Irvine DJ, Huppa JB, Davis MM. T cell killing does not require the formation of a stable mature immunological synapse. Nat Immunol. 2004;5(5):524–30. doi:10.1038/ni1058.

47. Riquelme E, Carreño LJ, González PA, Kalergis AM. The duration of TCR/pMHC interactions regulates CTL effector function and tumor-killing capacity. Eur J Immunol. 2009;39(8):2259–69. doi:10.1002/eji.200939341.

48. Amgen Inc. BLINCYTO®: FDA Package Insert. US Food Drug Adm. Website. 2021 Feb 25 Available from: https://www.accessdata.fda.gov/drugsatfda_docs/label/2018/125557s013lbl.pdf.

49. Stein AS, Schiller G, Benjamin R, Jia C, Zhang A, Zhu M, Zimmerman Z, Topp MS. Neurologic adverse events in patients with relapsed/refractory acute lymphoblastic leukemia treated with blinatumomab: management and mitigating factors. Ann Hematol. 2019;98(1):159–67. doi:10.1007/s00277-018-3497-0.

50. Shalabi H, Wolters PL, Martin S, Tamula MA, Roderick MC, Struemph K, Kane E, Yates B, Delbrook C, Mackall CL, et al. Systematic evaluation of neurotoxicity in children and young adults undergoing CD22 chimeric antigen receptor-T cell therapy. J Immunother (1991). 2018;41(7):350–58. Hagerstown Md 1997. doi:10.1097/CJI.0000000000000241.

51. Zhu Y, Shen R, Hao R, Wang S, Ho M. Highlights of antibody engineering and therapeutics 2019 in San Diego, USA: bispecific antibody design and clinical applications. Antib Ther. 2020;3 (2):146–54. doi:10.1093/abt/tbaa012.

52. Garfall AL, Lancaster E, Stadtmauer EA, Lacey SF, Dengel K, Ambrose DE, Chen F, Gupta M, Kulikovskaya I, Vogl DT, et al. Posterior reversible encephalopathy syndrome (pres) after infusion of anti-bcma car t cells (CART-BCMA) for multiple myeloma: successful treatment with cyclophosphamide. Blood. 2016;128 (22):5702–5702. doi:10.1182/blood.V128.22.5702.5702.

53. Cohen AD, Garfall AL, Stadtmauer EA, Melenhorst JJ, Lacey SF, Lancaster E, Vogl DT, Weiss BM, Dengel K, Nelson A, et al. B cell maturation antigen–specific CAR T cells are clinically active in multiple myeloma. J Clin Invest. 2019;129(6):2210–21. doi:10.1172/JCI126397.

54. Gust J, Hay KA, Hanafi L-A, Li D, Myerson D, Gonzalez-Cuyar LF, Yeung C, Liles WC, Wurfel M, Lopez JA, et al. Endothelial activation and blood-brain barrier disruption in neurotoxicity after adoptive immunotherapy with CD19 CAR-T Cells. Cancer Discov. 2017;7(12):1404–19. doi:10.1158/2159-8290.CD-17-0698.

55. Siegler EL, Kenderian SS. Neurotoxicity and cytokine release syndrome after chimeric antigen receptor t cell therapy: insights into mechanisms and novel therapies. Front Immunol. 2020;11. doi:10.3389/fimmu.2020.01973.

56. Pannu KK, Joe ET, Iyer SB. Performance evaluation of quantiBRITE phycoerythrin beads. Cytometry. 2001;45:250–58.